International Journal of Nanomedicine

Dovepress
open access to scientific and medical research

Open Access Full Text Article

ORIGINAL RESEARCH

Preparation, characterization, and in vitro osteoblast functions of a nano-hydroxyapatite/polyetheretherketone biocomposite as orthopedic implant material

This article was published in the following Dove Press journal:
International Journal of Nanomedicine
18 August 2014
Number of times this article has been viewed

Rui Ma[1]
Songchao Tang[2]
Honglue Tan[1]
Wentao Lin[1]
Yugang Wang[1]
Jie Wei[2]
Liming Zhao[2]
Tingting Tang[1]

[1]Shanghai Key Laboratory of Orthopedic Implants, Department of Orthopedic Surgery, Shanghai Ninth People's Hospital, Shanghai Jiao Tong University School of Medicine, [2]Key Laboratory for Ultrafine Materials of Ministry of Education and The State Key Laboratory of Bioreactor Engineering, East China University of Science and Technology, Shanghai, People's Republic of China

Correspondence: Tingting Tang
Shanghai Key Laboratory of Orthopedic Implants, Department of Orthopedic Surgery, Shanghai Ninth People's Hospital, Shanghai Jiao Tong University School of Medicine, Shanghai 200011, People's Republic of China
Tel +86 21 2327 1133
Fax +86 21 6313 7020
Email tingtingtang@hotmail.com

Liming Zhao
Key Laboratory for Ultrafine Materials of Ministry of Education and The State Key Laboratory of Bioreactor Engineering, East China University of Science and Technology, Shanghai 200237, People's Republic of China
Tel +86 021 64251308
Fax +86 021 64251358
Email slamdunk_86@163.com

Abstract: A bioactive composite was prepared by incorporating 40 wt% nano-hydroxyapatite (nHA) into polyetheretherketone (PEEK) through a process of compounding, injection, and molding. The mechanical and surface properties of the nHA/PEEK composite were characterized, and the in vitro osteoblast functions in the composite were investigated. The mechanical properties (elastic modulus and compressive strength) of the nHA/PEEK composite increased significantly, while the tensile strength decreased slightly as compared with PEEK. Further, the addition of nHA into PEEK increased the surface roughness and hydrophilicity of the nHA/PEEK composite. In cell tests, compared with PEEK and ultra-high-molecular-weight polyethylene, it was found that the nHA/PEEK composite could promote the functions of MC3T3-E1 cells, including cell attachment, spreading, proliferation, alkaline phosphatase activity, calcium nodule formation, and expression of osteogenic differentiation-related genes. Incorporation of nHA into PEEK greatly improved the bioperformance of PEEK. The nHA/PEEK composite might be a promising orthopedic implant material.

Keywords: polyetheretherketone, nano-hydroxyapatite, biocomposite, osteoblast functions, orthopedic implant material

Introduction

Hydroxyapatite (HA) ceramics with good biocompatibility and bioactivity have been widely used in clinical applications as bone-repairing materials that can bone-bond with living tissues.[1,2] However, due to its brittleness and fatigue failure, HA has been restricted in low load-bearing sites as bone repairing substitute.[3] Biomedical polymers, such as polyethylene (PE), polyamide (PA), Poly(ε-caprolactone) (PCL), poly(lactic acid) (PLA), poly(glycolic acid) (PGA), and poly(lactic-co-glycolic acid) (PLGA), have been used to fabricate different types of bone implant and tissue engineering scaffolds, owing to their good biocompatibility and malleable nature.[4–6] Nevertheless, none of these mentioned polymers is bioactive, which means that the newly formed bone tissues cannot bond tightly to the polymer surfaces.

To obtain bone implant materials with good bioactivity and the appropriate mechanical properties, the introduction of HA into polymers to fabricate inorganic/organic composites has been highlighted.[7–9] In this respect, HA-reinforced PE composite has been successfully developed for clinical application.[10] Following the concept of incorporating bioactive materials into polymers to increase the

bioactivity and mechanical properties of polymers, many composites containing bioactive materials (such as bioglass, HA, and tricalcium phosphate) and polymers (such as PA, PLA, and PCL) have been developed to prepare bone substitutes.[11–13]

"Polyetheretherketone" (PEEK) is a bone-implant material currently used in orthopedic applications.[14] Although PEEK has good biocompatibility and mechanical properties, its lack of bioactivity may limit its use in bone-repair applications.[15] Previous studies have reported that the addition of micron-sized HA into PEEK may improve the bioactivity of the resultant HA/PEEK composite, and that the bioactivity of the composite seems to increase with increasing HA content.[16–18] Li et al fabricated a nano-hydroxyapatite (nHA)-incorporated PEEK composite by powder processing and sintering, and their results suggested that the composite possessed good bioactivity and biocompatibility.[19]

To the best of our knowledge, no previous studies have reported the in vitro osteoblast responses (such as cell attachment, spreading, proliferation, and osteogenic differentiation of a pre-osteoblastic cell line [MC3T3-E1]) to the nHA/PEEK composite. In this study, nHA/PEEK composite was fabricated by incorporating nHA into a PEEK matrix through a process of compounding, injection, and molding. The mechanical properties, surface morphology, chemical composition, surface roughness, and hydrophilicity of the composite were characterized. The in vitro osteoblast functions of the composite were studied by detecting cell attachment, spreading, proliferation, and osteogenic differentiation of MC3T3-E1 cells.

Materials and methods

Preparation of nHA

Calcium nitrate ($Ca(NO_3)_2 \cdot 4H_2O$; Sigma-Aldrich, St Louis, MO, USA) and ammonium phosphate ($(NH_4)_3PO_4 \cdot 3H_2O$; Sigma-Aldrich) were separately dissolved in aqueous solution. The calcium nitrate solution was dropped slowly into the ammonium phosphate solution while the solution was stirred and heated to 70°C. The pH value of the solution was maintained between 10 and 12 by adding ammonium hydroxide (NH_4OH; Sigma-Aldrich). The chemical reaction formula was:

$$10\,Ca(NO_3)_2 + 6\,(NH_4)_3PO_4 + 2\,NH_4OH \xrightarrow{pH>10} Ca_{10}(PO_4)_6(OH)_2 + 20\,NH_4NO_3$$

When the reaction ended, nHA precipitate was obtained and thoroughly washed with deionized water, after which dimethylformamide (DMF; Sigma-Aldrich) was added gradually. The water in the precipitate solution was removed above 100°C; thus, the solvent became essentially DMF. Finally, the temperature was increased to 120°C and held for 2 hours. This procedure produced nHA, which was finally dried at 100°C for 12 hours to obtain nHA powder. The size and morphology of the nHA particles were characterized by transmission electron microscopy (TEM) using a JEM-100CX transmission electron microscope (JEOL, Tokyo, Japan).

Preparation of nHA/PEEK composite

PEEK powder with a mean particle size of 20 μm was obtained from Victrex Manufacturing Ltd (Rotherham, UK). A process involving compounding, injection, and molding was used to prepare the nHA/PEEK samples containing 0, 20, 40, and 60 wt% nHA content. The PEEK and nHA powders were compounded in a QM-3B High-Speed Vibrating Ball Mill (Nanjing T-Bota Scietech Instruments & Equipment Co Ltd, Nanjing, People's Republic of China) at a mixing speed of 500 rpm for 1 hour. Following this, the mixtures were then dried at 150°C for 24 hours. The samples were produced using a Battenfeld BA-300/050CD injection-molding machine (Awans, Belgium) at an injecting and molding temperature of 380°C.

"Ultra-high-molecular-weight polyethylene" (UHMWPE) is a commonly used prosthesis material in artificial hip and knee joints, so UHMWPE was chosen to serve as a control in cell tests. A UHMWPE slab with a molecular weight of 2 million was purchased from Röchling Engineering Plastics Ltd. (Munich, Germany). All samples were cut into 2 mm thick disks with diameters of 15 or 34 mm.

Mechanical properties

The mechanical properties (elastic modulus, tensile strength, and compressive strength) of the samples were measured using an Instron 5,567 material testing machine (Norwood, MA, USA) at a crosshead speed of 0.1 $mm \cdot min^{-1}$ according to ASTM International standard D790. The average of five readings for each sample was presented. All measurements were made in air at room temperature. By evaluating the mechanical properties of the nHA/PEEK composites with different nHA contents, we determined the optimal nHA content was 40 wt%, so this was selected to perform the other experiments in this study.

Surface morphology and chemical composition

The surface morphology and chemical composition of the nHA/PEEK composites were characterized by scanning electron microscopy (SEM; S-4800, Hitachi, Tokyo, Japan) and X-ray diffraction (XRD; Geigerflex, Rigaku Co, Akishima, Japan) with Cu Kα radiation (1.5405 Å).

Surface roughness and hydrophilicity

The surface roughness was measured as the average roughness (Ra) and root mean square roughness (Rq) using a HommelWerke T1000 surface roughness tester (Braunschweig, Germany). To determine the surface hydrophilicity, the sessile drop method was employed to measure the static water contact angle, using distilled water as the media, on a Ramé-Hart 290 Automated Goniometer/Tensiometer (Succasunna, NJ, USA) at ambient temperature. Five measurements were taken on different parts of each sample.

Cell culture

"MC3T3-E1" is a mouse pre-osteoblast cell line derived from mouse calvaria, and was chosen for this research to study the interaction between cells and materials in vitro. MC3T3-E1 cells were cultured in Dulbecco's Modified Eagle's Medium (DMEM) supplemented with 10% fetal bovine serum (FBS), 1% penicillin (100 $U \cdot mL^{-1}$), and streptomycin sulfate (100 $mg \cdot mL^{-1}$), all from Thermo Fisher Scientific (Waltham, MA, USA) at 37°C in a humidified atmosphere of 5% CO_2 and 95% air. The culture medium was changed every 3 days. For all the cell experiments, samples of the nHA/PEEK composite with 40 wt% nHA (Φ 15 mm) were used, and the PEEK and UHMWPE samples were used as controls.

Cell attachment

To study the attachment of MC3T3-E1 cells on the material surfaces, cell counting kit-8 (CCK-8) assay was performed to analyze the numbers of attached cells on material surfaces cultured for 6, 12, and 24 hours. Before seeding the cells, three disks for each group were put into the wells of a Costar 24-well plate (Corning Incorporated, NY, USA). The cell suspension was seeded into each well at a density of 3×10^4 viable cells per cm^2 of sample, with DMEM as a blank control. The culture plates were incubated at 37°C in a humidified atmosphere of 5% CO_2. At each time point, the samples were gently rinsed with phosphate-buffered saline (PBS) to remove the unattached cells then transferred to a new 24-well plate, and 50 μL CCK-8 solution (Dojindo Molecular Technologies Inc., Kumamoto, Japan) was added to each well. The plates were then incubated for 3 hours. At the end of this period, 100 μL of the supernatant was transferred into a 96-well plate. The plates were then read at 450 nm (with 620 nm as the reference wavelength) using a Synergy HT microplate reader (Bio-Tek Instruments Ltd, Winooski, VT, USA). The mean optical density (OD) obtained from the blank control was subtracted from the ODs of the test groups.

Cell spreading

Cell spreading was investigated by detecting the filamentous actin of the cytoskeleton of MC3T3-E1 cells. After 24 hours of incubation, the samples were washed gently three times with PBS to remove the unattached cells. Then the cells on the samples were fixed with 4% paraformaldehyde for 15 minutes at room temperature and permeabilized with 0.1% Triton X-100 in PBS for 10 minutes. After washing three times with PBS, the cells were stained with rhodamine-phalloidin (5 $units \cdot mL^{-1}$; Biotium, Hayward, CA, USA) for 30 minutes and then washed three times with PBS. The cytoskeleton was visualized by confocal laser scanning microscopy using a Leica Microsystems TCS SP2 (Heidelberg, Germany).

Cell spreading was also observed with SEM. After 24 hours, the cells on the samples were fixed with 2.5% glutaraldehyde for 15 minutes before being washed gently three times with PBS. Then the cells were dehydrated with gradient ethanol (30%, 50%, 70%, 90%, 100%, and 100% for 10 minutes each time). Finally, all the samples were air-dried at room temperature, sputter-coated with gold, and observed with SEM.

Cell proliferation

CCK-8 assay was used to study the proliferation of the MC3T3-E1 cells on the samples. The detailed procedures were nearly identical to the procedures for the cell attachment test. The differences were that the seeding density of the cells was 1×10^4 viable cells per cm^2, and the time points were 1, 3, and 7 days. Similar to the cell seeding procedures of the cell proliferation test, the cells on the samples were also stained with 4,6-diamidino-2-phenylindole (DAPI, 0.1 $\mu g \cdot mL^{-1}$; Sigma-Aldrich) for 15 minutes after being cultured for 1, 3, and 7 days. After DAPI staining, the cells were observed using a fluorescence microscope (Leica AF 6000, Heidelberg, Germany). For quantitative analysis of DAPI staining, five representative images were selected for each group and the cells numbers were counted using GraphPad Prism® software (v 5.0; La Jolla, CA, USA). The MC3T3-E1 cells cultured for 3 and 7 days on the samples were also observed by SEM.

Cell culture of inductive osteogenesis

Specimens (Φ 34 mm) were placed into a six-well plate then seeded with MC3T3-E1 cells at a density of 3×10^4 viable cells per cm^2. After co-incubation with the samples for 24 hours, the culture medium was changed to the osteogenic inductive medium, which contained DMEM supplemented with 10% FBS, 1% penicillin (100 $U\cdot mL^{-1}$), streptomycin sulfate (100 $mg\cdot mL^{-1}$), 100 nm dexamethasone (Sigma-Aldrich), 50 $\mu g\cdot mL^{-1}$ ascorbic acid (Sigma-Aldrich), and 10 mm β-glycerophosphate sodium (Sigma-Aldrich). The osteogenic inductive medium was replaced every 2 days.

Alkaline phosphatase (*ALP*) staining and *ALP* activity assay

After 7, 10, and 14 days of culturing in the osteogenic inductive medium, *ALP* staining was performed following our previously published procedure.[20] *ALP* activity was determined by quantifying the amount of p-nitrophenol, the yellow-colored end product of hydrolysis of p-nitrophenyl phosphate, using an *ALP* microplate test kit (Nanjing Jiancheng Bioengineering Institute, Nanjing, People's Republic of China). The quantity of *ALP* in the cell lysates was measured at 405 nm using the Synergy HT microplate reader, while the total protein content was determined using a BCA protein assay kit (Thermo Fisher Scientific) according to the provided protocol. Finally, the *ALP* activity was normalized to the corresponding total protein content.

Alizarin-red staining and quantitative analysis

After osteogenic induction for 21 and 28 days, the samples were washed three times with PBS and fixed in 4% paraformaldehyde for 15 minutes before being stained with 1% alizarin-red solution (pH 4.2; Sigma-Aldrich) for 45 minutes at room temperature. Next, the samples were washed with deionized water until the deionized water did not appear orange, then dried at 37°C.

Additionally, the samples with no cells were stained with 1% alizarin-red solution as just described. For the quantitative analysis of alizarin-red staining, the orange dye was dissolved in 10% cetylpyridinium chloride (Sigma-Aldrich) in 10 mm sodium phosphate (pH 7.0; Sigma-Aldrich), and the OD values were measured at 620 nm using the microplate reader.[21] The mean ODs obtained from the samples with no cells were subtracted from the ODs of each test group.

Expression of osteogenic differentiation-related genes

The expression of MC3T3-E1 osteogenic differentiation-related genes on the samples was quantitatively determined by real-time polymerase chain reaction (PCR). Messenger ribonucleic acid (mRNA) levels of mouse *ALP, type I collagen* (*COL1*), *osteopontin* (*OPN*), and *osteocalcin* (*OC*) were evaluated and normalized to the transcript levels of the housekeeping gene *β-actin*. The sequences of the forward and reverse primers, and the lengths of the products for the osteogenic differentiation-related genes are shown in Table 1. The quantification of gene expression was based on the cycle threshold (CT) values of each measurement. After osteogenic induction for 7, 14, and 21 days, the total RNA was collected from the cell lysates using Trizol reagent (Invitrogen, Carlsbad, CA, USA) according to the manufacturer's protocol. One microgram of the total RNA from each sample was added to the oligo$(dT)_{18}$ primers, heated at 65°C for 5 minutes then cooled on ice for 1 minute before reaction buffer, RNase-inhibitor, deoxy-ribonucleoside triphosphate (dNTP), and reverse transcriptase were added according to RevertAid First Strand cDNA Synthesis Kit (Thermo Fisher Scientific) protocol. Quantitative real-time PCR was undertaken using a SYBR premix EX Taq™ PCR kit (Takara Biotechnology Co Ltd, Dalian, People's Republic of China). PCR amplification was performed in triplicate for each group in an independent PCR amplification and repeated in two independent experiments.

Statistical analysis

All data are presented as the means ± standard deviations. All experiments were repeated three times. Statistical analysis was performed using a two-way analysis of variance (ANOVA) test to determine the presence of any significant differences between different groups, and multiple comparisons were

Table 1 Primers used in this study

Target gene	Primer sequence (5′ → 3′)	Product length (bp)
ALP	F: GGGCATTGTGACTACCACTCG	104
	R: CCTCTGGTGGCATCTCGTTAT	
COL1	F: AACAGTCGCTTCACCTACAGC	96
	R: GGTCTTGGTGGTTTTGTATTCG	
OPN	F: CTTTCACTCCAATCGTCCCTAC	165
	R: CCTTAGACTCACCGCTCTTCAT	
OC	F: GGACCATCTTTCTGCTCACTCTG	130
	R: TTCACTACCTTATTGCCCTCCTG	
β-actin	F: GAGACCTTCAACACCCCAGC	263
	R: ATGTCACGCACGATTTCCC	

Abbreviations: *ALP*, alkaline phosphatase; bp, base pair; *COL1*, type I collagen; F, forward; *OC*, osteocalcin; *OPN*, osteoprotein; R, reverse.

performed using the least significant difference (LSD) test to determine any significant differences between each pair of groups. $P<0.05$ was considered statistically significant, and $P<0.01$ was considered highly statistically significant. All statistical analyses were performed using SPSS software (v 13.0; IBM Corp, Armonk, NY, USA).

Results

TEM of nHA

Figure 1 is a TEM image of nHA. It can be seen that the prepared nHA exhibited a rod-like morphology with an average length of 80 nm and diameter of 10 nm.

Mechanical properties of the composite

Table 2 shows the mechanical properties of the nHA/PEEK composite with different contents of nHA. The elastic modulus and compressive strength of the composite increased with increasing nHA content from 0 to 40 wt%. The highest nHA content (60 wt%) yielded a lower elastic modulus (3.9 MPa) and compressive strength (89 MPa) than the composite containing 40 wt% nHA. The composite containing 40 wt% nHA resulted in the highest elastic modulus (4.6 MPa) and compressive strength (160 MPa), indicating that the addition of nHA into PEEK improved the mechanical properties to a point. Further, the tensile strength of the composites decreased slightly as nHA content increased and was lower than that of PEEK.

SEM and XRD of the composite

Figure 2 presents an SEM image and the XRD pattern of the nHA/PEEK composite. Many high-electron-density nHA particles were found uniformly distributed on the composite's surface (Figure 2A). Figure 2A presents the XRD pattern of the nHA/PEEK composite. The diffraction peaks of the composite at around $2\theta = 25.5°$, 32°, 33°, 40°, and 49.5° ascribe to the characteristic peaks of HA,[22] while the two peaks at around $2\theta = 21°$ and 22.5° are the characteristic peaks of PEEK.[23] The results indicate that the composite contained both the nHA and PEEK.

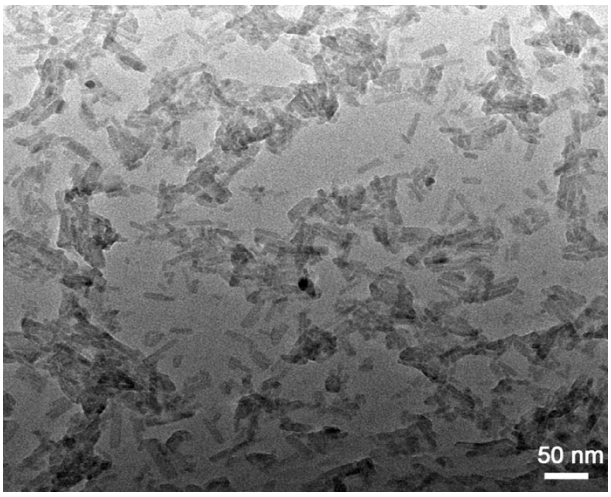

Figure 1 Transmission electron microscope image of nano-hydroxyapatite.

Table 2 Mechanical properties of the nano-hydroxyapatite/polyetheretherketone (nHA/PEEK) composite with different nano-hydroxyapatite (nHA) contents

Samples	Elastic modulus (GPa)	Tensile strength (MPa)	Compressive strength (MPa)
PEEK	2.20±0.17	84.0±1.9	112.0±2.2
20 wt% nHA/PEEK	3.40±0.20	81.0±2.4	137.0±3.0
40 wt% nHA/PEEK	4.60±0.12	75.0±2.7	160.0±3.1
60 wt% nHA/PEEK	3.90±0.23	58.0±2.5	89.0±4.5

Note: The data are presented as means ± standard deviations.
Abbreviation: PEEK, polyetheretherketone.

Surface roughness and the hydrophilicity of the composite

Table 3 shows the surface roughness of the nHA/PEEK composite and PEEK. The Ra and Rq of the composite were 0.118 and 0.183, and those of PEEK were 0.063 and 0.095, respectively. The results indicate that, compared with PEEK, the Ra and Rq of the composite increased by 87% and 93%, respectively. Figure 3 shows the results of the water contact angles of the nHA/PEEK composite and PEEK, which were 51° and 74°, respectively. These results indicate that the hydrophilicity of the composite was significantly improved compared with PEEK ($P<0.01$).

Cell attachment

Figure 4 illustrates the numbers of attached cells on the nHA/PEEK composite, PEEK, and UHMWPE. The number of cells attached to the composite was significantly higher than the numbers on PEEK and UHMWPE after 12 and 24 hours ($P<0.05$). This indicates that the addition of nHA into PEEK improved cell attachment on the composite.

Cell spreading

Figure 5A shows the cytoskeleton of MC3T3-E1 cells observed by confocal laser scanning microscopy after culture for 24 hours. The cells on the nHA/PEEK composite exhibit clustering, confluent, and multilayer morphology with more actin filaments linking adjacent cells, whereas the cells on PEEK and UHMWPE appear dispersive and monolayer, with fewer actin filaments. Figure 5B presents the SEM images

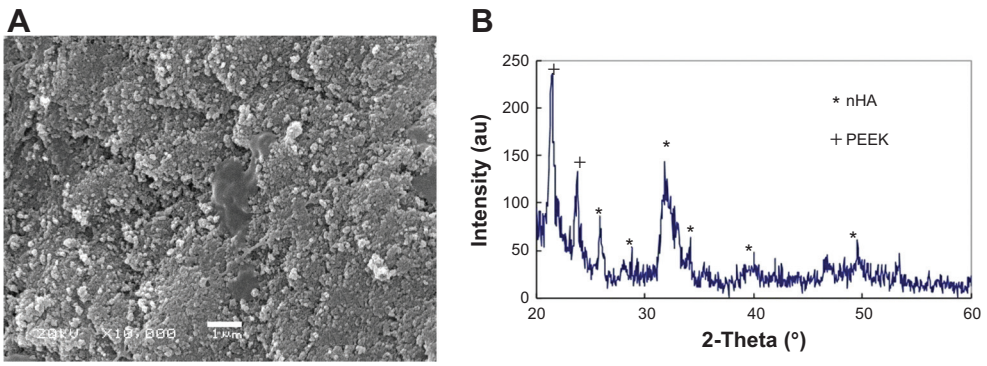

Figure 2 Scanning electron microscope image (**A**) and X-ray diffraction pattern (**B**) of the nano-hydroxyapatite (nHA)/polyetheretherketone (PEEK) composite.

of MC3T3-E1 cells after 24 hours. The cells on the nHA/PEEK composite surface spread well; the cells were polygonal, with numerous pseudopods anchored to the material's surface. In contrast, on PEEK and UHMWPE, cell spreading appeared less efficient; the cells were rod-like, with fewer pseudopods.

Cell proliferation

Figure 6 presents the proliferation of MC3T3-E1 cells cultured on the nHA/PEEK composite, PEEK, and UHMWPE as determined by CCK-8 assay. The cell numbers on the composite increased significantly from 1 to 7 days. In addition, the cell numbers on PEEK and UHMWPE increased obviously from 3 to 7 days and from 1 to 3 days, respectively ($P<0.05$). However, the cell numbers on PEEK and UHMWPE exhibited no significant increase from 1 to 3 days and from 3 to 7days, respectively ($P>0.05$). Figure 6B indicates that the cells on the composite exhibited a higher relative proliferation rate than on PEEK at 3 days and UHMWPE at 7 days ($P<0.05$). Further, the relative proliferation rate of MC3T3-E1 cells on the nHA/PEEK composite was a little less than on PEEK at 7 days, but no significant difference existed between them ($P>0.05$).

The qualitative and quantitative analysis of DAPI staining of MC3T3-E1 cells cultured on the nHA/PEEK composite, PEEK, and UHMWPE is shown in Figure 7. The results indicate that more cells grew on the composite than on PEEK and UHMWPE at each time point ($P<0.01$).

Figure 8 presents the SEM images of cells cultured on the samples at 3 and 7 days. The cells on the nHA/PEEK composite spread better than on PEEK and UHMWPE at 3 days. Further, the cells on the composite and PEEK spread well and covered almost the entire material's surface at 7 days, whereas the cells on UHMWPE were in a poor state and exhibited no apparent proliferative trend from 3 to 7 days.

ALP staining and *ALP* activity

Figure 9A illustrates the *ALP* staining of the MC3T3-E1 cells cultured on the samples. The *ALP* staining became stronger with induction time on all samples, and the staining on the nHA/PEEK composite was considerably stronger than on PEEK and UHMWPE at each time point. Figure 9B shows the *ALP* activity of the MC3T3-E1 cells cultured on the samples. The *ALP* activity on the composite was significantly higher than on PEEK and UHMWPE on days 7, 14, and 21.

Table 3 Surface roughness of the nano-hydroxyapatite/polyetheretherketone (nHA/PEEK) composite and polyetheretherketone (PEEK)

Sample	Ra (μm)	Rq (μm)
PEEK	0.063±0.012	0.095±0.024
nHA/PEEK composite	0.118±0.032*	0.183±0.053*

Note: *$P<0.01$ compared with PEEK. The data are presented as means ± standard deviations.
Abbreviations: Ra, average roughness; Rq, root mean square roughness.

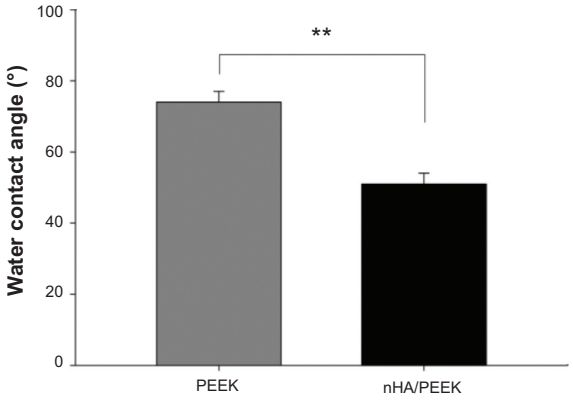

Figure 3 Water contact angles of the nano-hydroxyapatite/polyetheretherketone (nHA/PEEK) composite and polyetheretherketone (PEEK).
Note: **Significant difference compared with PEEK ($P<0.01$).
Abbreviations: PEEK, polyetheretherketone; nHA/PEEK, nano-hydroxyapatite/polyetheretherketone.

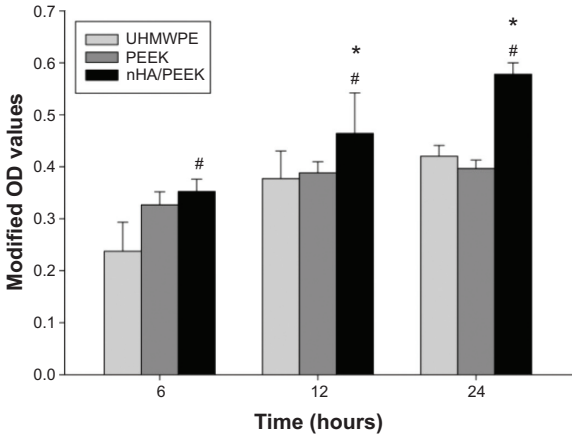

Figure 4 Cell attachment on the samples assessed by cell counting kit-8 assay.
Notes: *Significant difference compared with PEEK ($P<0.05$); #significant difference compared with UHMWPE ($P<0.05$).
Abbreviations: nHA/PEEK, nano-hydroxyapatite/polyetheretherketone; OD, optical density; PEEK, polyetheretherketone; UHMWPE, ultra-high-molecular-weight polyethylene.

Alizarin-red staining and quantitative analysis

Figure 10A shows the alizarin-red staining of the MC3T3-E1 cells cultured on the samples. The alizarin-red staining on the nHA/PEEK composite was clearly stronger than on PEEK and UHMWPE at 21 and 28 days. Figure 10B shows the quantitative analysis of the alizarin-red staining of the MC3T3-E1 cells on the samples. The results indicate that the calcium nodule-formation of the cells on the composite was significantly more than on PEEK and UHMWPE at 21 and 28 days ($P<0.01$).

Expression of osteogenic differentiation-related genes

Figure 11 shows the expression of osteogenic differentiation-related genes of MC3T3-E1 cells cultured on the samples. The mRNA of *ALP* for the composite was obviously higher than PEEK and UHMWPE at 7 and 14 days, and the mRNA of *OC* for the composite was obviously higher than PEEK and UHMWPE at 21 days. Moreover, the mRNA of *COL1* for the composite was obviously higher than PEEK and UHMWPE at 14 and 21 days, and the mRNA of *OPN* for the composite was obviously higher than UHMWPE at 14 and 21 days.

Discussion

In this study, a bioactive composite of nHA/PEEK was prepared by introducing nHA into PEEK using a process of compounding, injection, and molding. The SEM and XRD

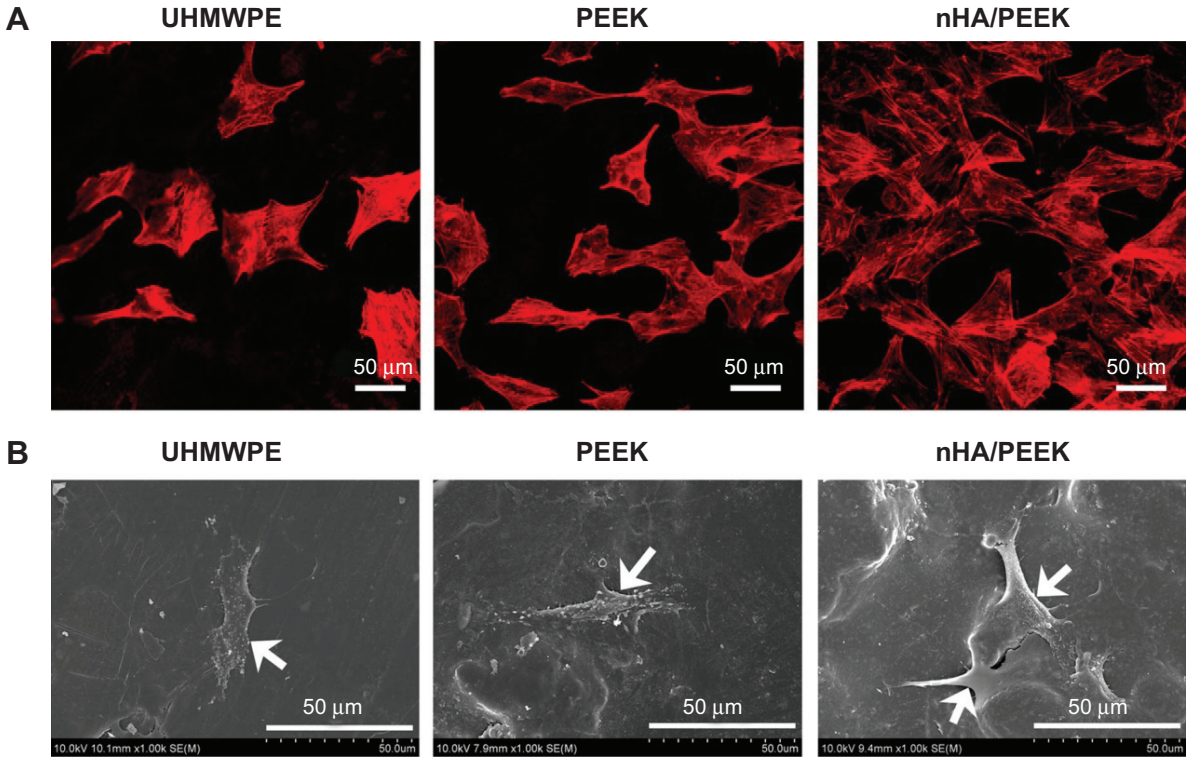

Figure 5 Cell spreading on the samples at 24 hours, as observed by (**A**) confocal laser scanning microscope and (**B**) scanning electron microscope.
Note: Arrows indicate cells.
Abbreviations: nHA/PEEK, nano-hydroxyapatite/polyetheretherketone; PEEK, polyetheretherketone; UHMWPE, ultra-high-molecular-weight polyethylene.

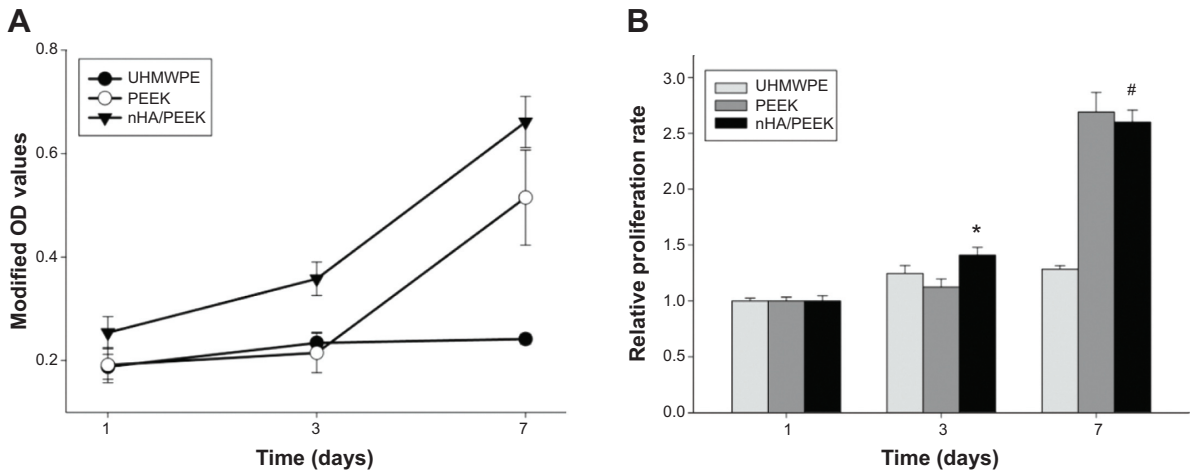

Figure 6 Cell proliferation on the samples assessed by cell counting kit-8 assay.
Notes: (**A**) proliferative tendency from 1 to 7 days; (**B**) relative proliferation rate. The modified optical densities at 3 and 7 days were normalized to the values at 1 day. *Significant difference compared with PEEK ($P<0.05$); #significant difference compared with UHMWPE ($P<0.05$).
Abbreviations: nHA/PEEK, nano-hydroxyapatite/polyetheretherketone; OD, optical density; PEEK, polyetheretherketone; UHMWPE, ultra-high-molecular-weight polyethylene.

results show that the nHA particles were uniformly distributed on the PEEK matrix.

After the incorporation of nHA into PEEK, the elastic modulus and compressive strength mechanical properties of the nHA/PEEK composite (from 0 to 40 wt%) increased obviously, while the tensile strength decreased slightly when compared with PEEK. In the composite system, the compressive strength and elastic modulus of the composite containing 40 wt% nHA were significantly higher than in those containing 20 wt% and 60 wt%, suggesting that a weight ratio of about 40 wt% would be optimal. Composites containing a high nHA content (for example, 60 wt%) resulted in a dramatic reduction in the mechanical strength of the composite. Therefore, the composite with 40 wt% nHA was chosen for other investigations in this study.

The biocompatibility of a biomaterial is affected by its surface characteristics, such as surface roughness and hydrophilicity.[24] In this study, the results revealed that the Ra and Rq of the nHA/PEEK composite were 87% and 93%, respectively, greater than those of PEEK, indicating that the incorporation of nHA into PEEK obviously increased the surface roughness of the composite. The rougher surface of implant biomaterials may exert a positive influence on the proliferation and differentiation of osteoblasts.[25,26]

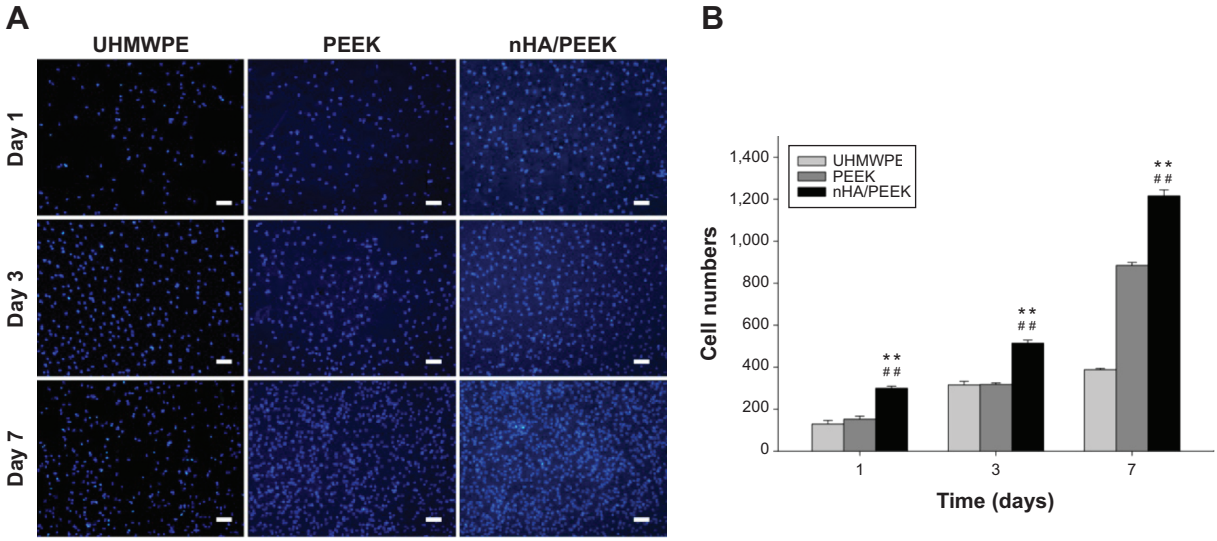

Figure 7 Cell proliferation in the samples assessed by 4,6-diamidino-2-phenylindole (DAPI) staining.
Notes: (**A**) MC3T3-E1 cells stained with DAPI after 1, 3, and 7 days; (**B**) quantitative analysis of DAPI staining. **Significant difference compared with PEEK ($P<0.01$); ##significant difference compared with UHMWPE ($P<0.01$); scale bar =50 μm.
Abbreviations: nHA/PEEK, nano-hydroxyapatite/polyetheretherketone; PEEK, polyetheretherketone; UHMWPE, ultra-high-molecular-weight polyethylene.

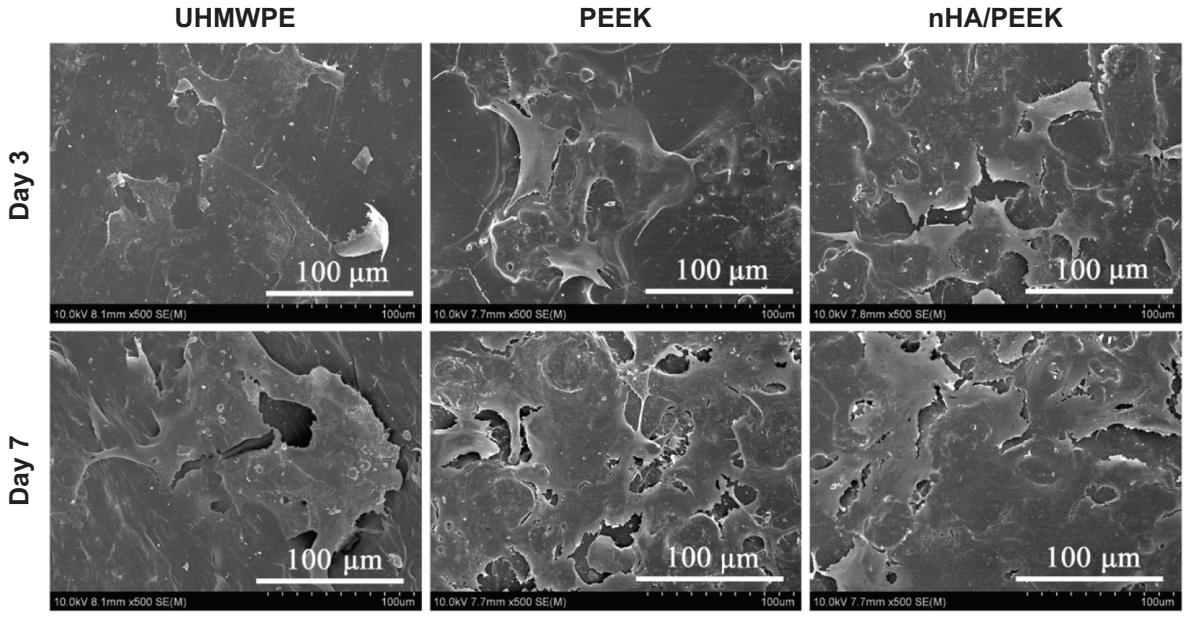

Figure 8 Scanning electron microscope images of MC3T3-E1 cells on the samples at 3 and 7 days.
Abbreviations: nHA/PEEK, nano-hydroxyapatite/polyetheretherketone; PEEK, polyetheretherketone; UHMWPE, ultra-high-molecular-weight polyethylene.

Hydrophilic testing revealed that the water contact angles of nHA/PEEK and PEEK were 51° and 74°, respectively, indicating that addition of nHA into PEEK enhanced the hydrophilicity of the composite. Contact angle depends on many factors, for instance, surface roughness, surface chemistry, and grain size.[27] Because nHA is more hydrophilic as an inorganic material than PEEK, and the nHA/PEEK composite is rougher than PEEK, the improvement in hydrophilicity seen with the nHA/PEEK composite may stem from changes in the surface roughness and chemistry,[27,28] which may have affected the functions of the osteoblasts in this study.

Cell attachment is the first step in the interaction of cells with substrate materials, which can affect cell growth and proliferation on the biomaterial surfaces.[29,30] It has been reported that the attachment of fibroblasts on the biomaterials is more evident on hydrophilic surfaces than hydrophobic ones.[31] In this study, the nHA/PEEK composite significantly promoted the attachment of the MC3T3-E1 cells compared with PEEK and UHMWPE, which may be due to the

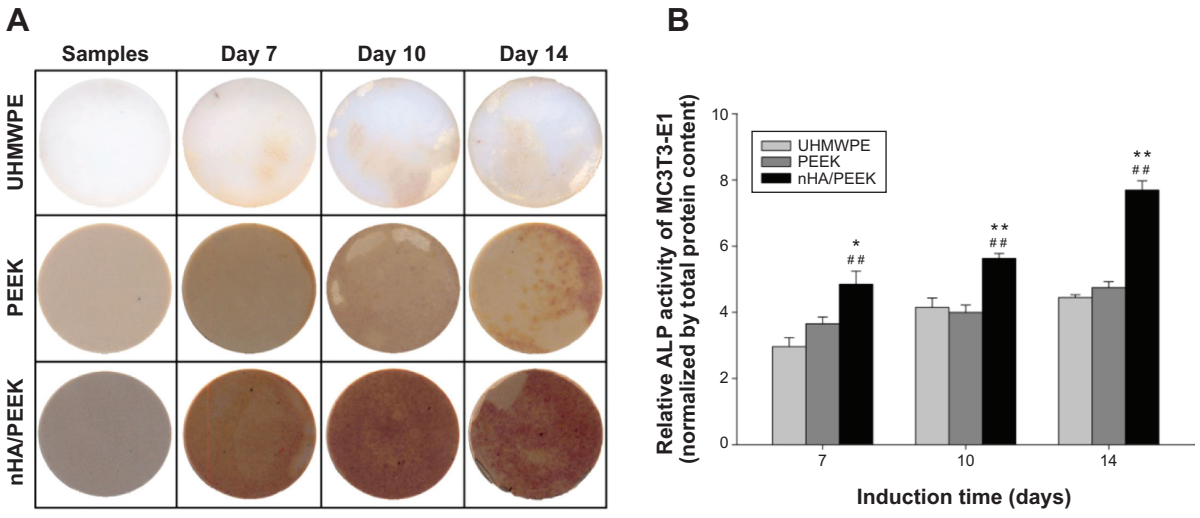

Figure 9 Alkaline phosphatase (*ALP*) staining and quantification of *ALP* activity on the samples after osteogenic induction for 7, 10, and 14 days.
Notes: (**A**) *ALP* staining on the samples; (**B**) quantitative analysis of *ALP* activity. *ALP* activity was normalized to the corresponding total protein content. *Significant difference compared with PEEK ($P<0.05$); **significant difference compared with PEEK ($P<0.01$); ##significant difference compared with UHMWPE ($P<0.01$).
Abbreviations: nHA/PEEK, nano-hydroxyapatite/polyetheretherketone; PEEK, polyetheretherketone; UHMWPE, ultra-high-molecular-weight polyethylene.

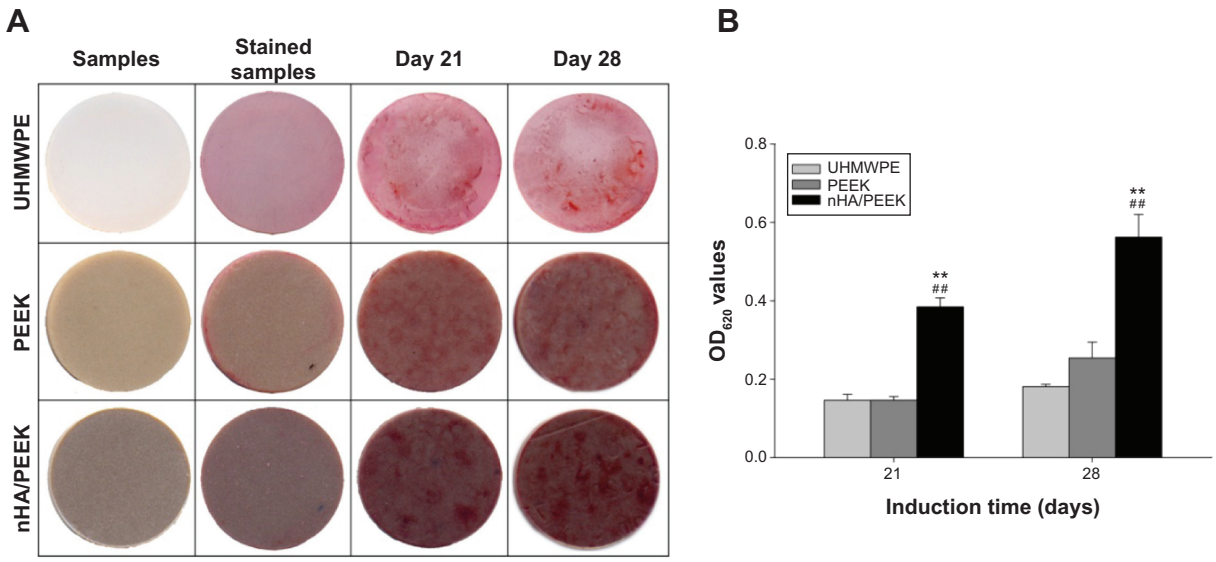

Figure 10 Alizarin-red staining and quantitative analysis of mineralization on the samples.
Notes: (**A**) samples, stained samples without cells, and stained samples with cells at 21 and 28 days; (**B**) colorimetric quantification of the extracellular matrix mineralization at 21 and 28 days. **Significant difference compared with PEEK ($P<0.01$); ##significant difference compared with UHMWPE ($P<0.01$).
Abbreviations: OD, optical density; nHA/PEEK, nano-hydroxyapatite/polyetheretherketone; PEEK, polyetheretherketone; UHMWPE, ultra-high-molecular-weight polyethylene.

composite's increased surface hydrophilicity and roughness. The nHA/PEEK composite possessed a hydrophilic surface that facilitated cell attachment, whereas PEEK had a relatively hydrophobic surface that limited cell attachment. Additionally, the surface roughness of the composite favored the adsorption of greater amounts of protein, thereby promoting the attachment of osteoblasts.[32] In this study, cells spread well on the composite, with more actin filaments and pseudopods compared with on PEEK and UHMWPE, indicating good biocompatibility and bioactivity. This could be attributed to the hydrophilic surface of the composite, and it has been reported that the actin fibers of fibroblasts are evident on hydrophilic surfaces than on hydrophobic ones.[31]

After attaching to the material surfaces, the MC3T3-E1 cells enter a proliferation stage. Our results show that the nHA/PEEK composite could promote the proliferation of MC3T3-E1 cells, as compared with PEEK and UHMWPE. Studies have shown that HA can stimulate the cell proliferation of human and animal osteoblasts.[33] Thus, the active effect on the cell proliferation of the composite was mainly attributed to the biological benefits of nHA. Further, the surface roughness and hydrophilicity of biomaterials have been reported to positively influence the proliferation potential of MG-63 cells (a human osteosarcoma cell line).[34] Therefore, the increased surface roughness and hydrophilicity of the composite also favored cell proliferation on the composite.

After attachment and proliferation, the cells on the biomaterial surfaces further differentiate to synthesize collagen and other proteins, and induce their own in vitro mineralization in certain culture medium conditions.[35] *ALP* is a marker for the early differentiation of osteoblasts; it regulates the inorganic phosphate metabolism by hydrolyzing phosphate esters and functions as a plasma membrane transporter for inorganic phosphates.[36] Alizarin-red staining is commonly used to detect the formation of calcium nodules (mineralization) – formed by osteoblasts in the late stage of differentiation – in osteoblast cultures.[37] In the present study, the MC3T3-E1 cells on the composite exhibited higher *ALP* activity and more calcium nodule-formation than PEEK and UHMWPE, indicating that the composite could promote the cell differentiation of MC3T3-E1 cells.

To further study osteogenic differentiation, real-time PCR was used to monitor the changes in the expression levels of osteogenic differentiation-related genes (*ALP*, *COL1*, *OPN*, and *OC*) of the MC3T3-E1 cells on the composite and the PEEK and UHMWPE controls. The MC3T3-E1 cells cultured on the composite exhibited a significantly higher expression of *ALP* at 7 and 14 days than on PEEK and UHMWPE, which was in accordance with the results of *ALP* activity quantification. *OC* expression on the composite was significantly higher than on PEEK and UHMWPE at 21 days, consistent with the results of the mineralization measured by quantification of alizarin-red staining. In addition, the composite exhibited higher expression of *COL1* at 14 and 21 days compared with PEEK and UHMWPE. These results indicate that the nHA/PEEK composite can promote

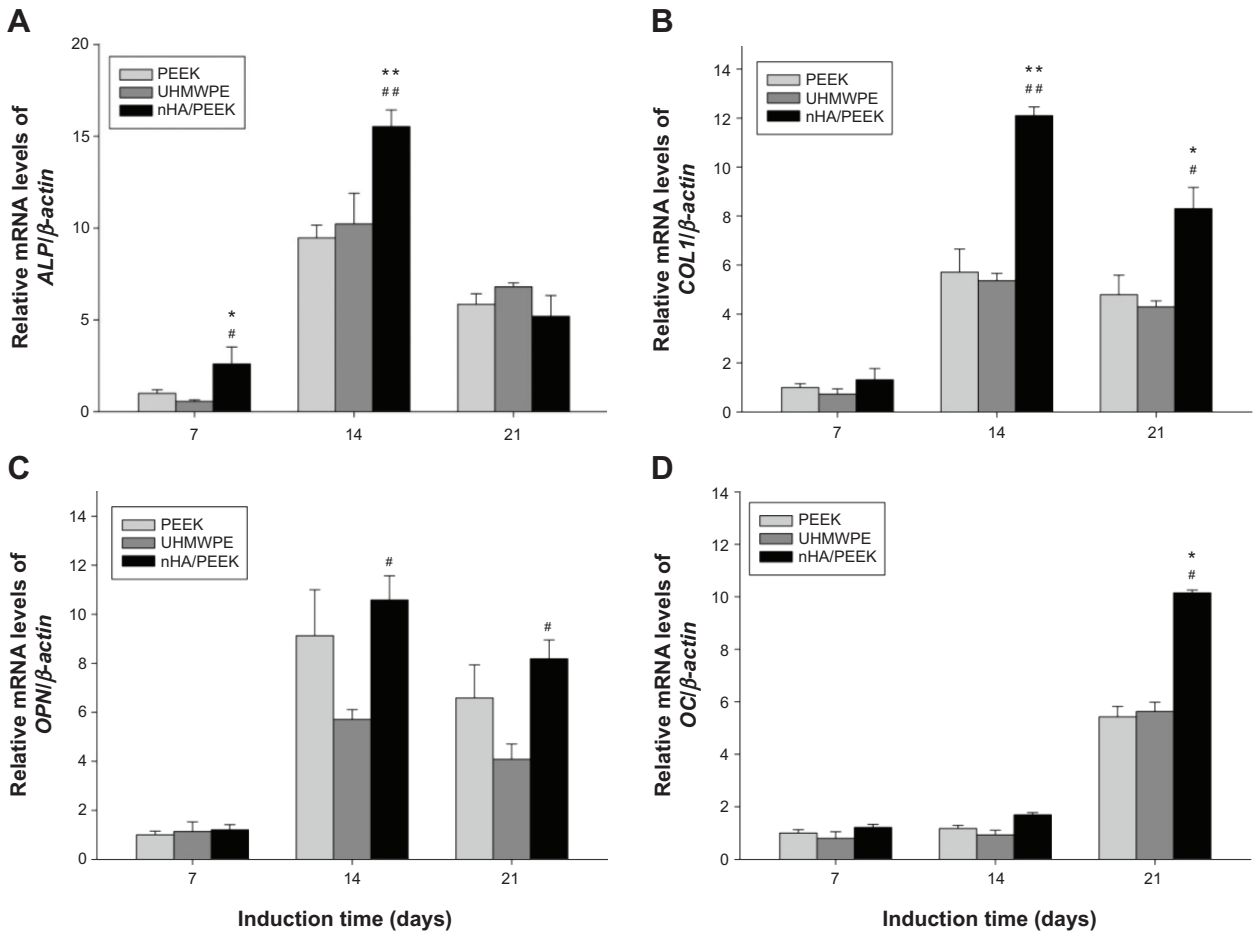

Figure 11 Expression of osteogenic differentiation-related genes of MC3T3-E1 cells on the samples assessed by real-time polymerase chain reaction.
Notes: (**A**) *ALP*, (**B**) *COL1*, (**C**) *OPN*, and (**D**) *OC*. The data shown are the mean expression relative to *β-actin* expression and are normalized with respect to the expression on PEEK at 7 days. *Significant difference compared with PEEK ($P<0.05$); **significant difference compared with PEEK ($P<0.01$); #significant difference compared with UHMWPE ($P<0.05$); ##significant difference compared with UHMWPE ($P<0.01$).
Abbreviations: *ALP*, alkaline phosphatase; *COL1*, type I collagen; mRNA, messenger ribonucleic acid; nHA/PEEK, nano-hydroxyapatite/polyetheretherketone; *OPN*, osteoprotein; *OC*, osteocalcin; PEEK, polyetheretherketone; UHMWPE, ultra-high-molecular-weight polyethylene.

the osteogenic differentiation of the MC3T3-E1 cells. HA is bioactive and can promote the osteogenic differentiation of osteoblasts,[33] especially nHA.[38] A study has reported that a rougher surface of the substrate material improves the differentiation of osteoblasts;[25] therefore, the promotion of the osteogenic differentiation of the MC3T3-E1 cells on the nHA/PEEK composite was mainly due to the biological benefits of nHA and the rougher surface of the composite.

Conclusion

In the study reported here, a bioactive composite of nHA/PEEK was prepared through a process of compounding, injection, and molding. The results show that nHA was uniformly distributed on the PEEK matrix, and the mechanical properties (elastic modulus and compressive strength) of the composite were significantly increased compared with those of PEEK. In addition, the surface roughness and hydrophilicity of the nHA/PEEK composite increased due to the introduction of nHA into PEEK. In the evaluation of the osteoblast functions on material surfaces, the nHA/PEEK composite was found to promote cell attachment, spreading, proliferation, and osteogenic differentiation with higher *ALP* activity, increase calcium nodule-formation, and generate higher expression levels of osteogenic differentiation-related genes compared with PEEK and UHMWPE. The bioactive nHA/PEEK composite may have potential in orthopedic applications.

Acknowledgments

This research was financially supported by the National Natural Science Foundation of China (numbers 31271015, 81271705, and 51173041) and the Shanghai Science and Technology Development Fund (numbers 13DZ2294000, 13JC1403900, 12nm0500400, and 12441903600).

Disclosure

The authors declare no conflicts of interest in this work.

References

1. McMahon RE, Wang L, Skoracki R, Mathur AB. Development of nanomaterials for bone repair and regeneration. *J Biomed Mater Res B Appl Biomater.* 2013;101(2):387–397.
2. Lee JS, Baek SD, Venkatesan J, et al. In vivo study of chitosan-natural nano hydroxyapatite scaffolds for bone tissue regeneration. *Int J Biol Macromol.* 2014;67:360–366.
3. Roeder RK, Converse GL, Kane RJ, Yue W. Hydroxyapatite-reinforced polymer biocomposites for synthetic bone substitutes. *JOM.* 2008;60(3): 38–45.
4. Zong C, Qian X, Tang Z, et al. Biocompatibility and bone-repairing effects: comparison between porous poly-lactic-co-glycolic acid and nano-hydroxyapatite/poly(lactic acid) scaffolds. *J Biomed Nanotechnol.* 2014;10(6):1091–1104.
5. Asti A, Gioglio L. Natural and synthetic biodegradable polymers: different scaffolds for cell expansion and tissue formation. *Int J Artif Organs.* 2014;37(3):187–205.
6. Baxter RM, Macdonald DW, Kurtz SM, Steinbeck MJ. Severe impingement of lumbar disc replacements increases the functional biological activity of polyethylene wear debris. *J Bone Joint Surg Am.* 2013; 95(11):e751–e759.
7. Aydin E, Planell JA, Hasirci V. Hydroxyapatite nanorod-reinforced biodegradable poly(L-lactic acid) composites for bone plate applications. *J Mater Sci Mater Med.* 2011;22(11):2413–2427.
8. Kim H, Kim HM, Jang JE, et al. Osteogenic Differentiation of Bone Marrow Stem Cell in Poly(Lactic-co-Glycolic Acid) Scaffold Loaded Various Ratio of Hydroxyapatite. *Int J Stem Cells.* 2013;6(1): 67–74.
9. Díez-Pascual AM, Naffakh M, Marco C, Ellis G, Gómez-Fatou MA. High-performance nanocomposites based on polyetherketones. *Prog Mater Sci.* 2012;57(7):1106–1190.
10. Di Silvio L, Dalby MJ, Bonfield W. Osteoblast behaviour on HA/PE composite surfaces with different HA volumes. *Biomaterials*. 2002; 23(1):101–107.
11. Zhang X, Chang W, Lee P, et al. Polymer-ceramic spiral structured scaffolds for bone tissue engineering: effect of hydroxyapatite composition on human fetal osteoblasts. *Plos One.* 2014;9(1):e85871.
12. Liu D, Zhuang J, Shuai C, Peng S. Mechanical properties' improvement of a tricalcium phosphate scaffold with poly-l-lactic acid in selective laser sintering. *Biofabrication.* 2013;5(2):025005.
13. Su J, Cao L, Yu B, et al. Composite scaffolds of mesoporous bioactive glass and polyamide for bone repair. *Int J Nanomedicine.* 2012;7: 2547–2555.
14. Kurtz SM, Devine JN. PEEK biomaterials in trauma, orthopedic, and spinal implants. *Biomaterials.* 2007;28(32):4845–4869.
15. Ma R, Tang T. Current strategies to improve the bioactivity of PEEK. *Int J Mol Sci.* 2014;15(4):5426–5445.
16. Ma R, Weng L, Bao X, Song S, Zhang Y. In vivo biocompatibility and bioactivity of in situ synthesized hydroxyapatite/polyetheretherketone composite materials. *J Appl Polym Sci.* 2013;127(4): 2581–2587.
17. Yu S, Hariram KP, Kumar R, Cheang P, Aik KK. In vitro apatite formation and its growth kinetics on hydroxyapatite/polyetheretherketone biocomposites. *Biomaterials.* 2005;26(15):2343–2352.
18. Converse GL, Yue W, Roeder RK. Processing and tensile properties of hydroxyapatite-whisker-reinforced polyetheretherketone. *Biomaterials.* 2007;28(6):927–935.
19. Li K, Yeung CY, Yeung KW, Tjong SC. Sintered hydroxyapatite/polyetheretherketone nanocomposites: mechanical behavior and biocompatibility. *Adv Eng Mater.* 2012;14(4):B155–B165.
20. Fan Q, Tang T, Zhang X, Dai K. The role of CCAAT/enhancer binding protein (C/EBP)-alpha in osteogenesis of C3H10T1/2 cells induced by BMP-2. *J Cell Mol Med.* 2009;13(8B):2489–2505.
21. Zhao L, Mei S, Chu PK, Zhang Y, Wu Z. The influence of hierarchical hybrid micro/nano-textured titanium surface with titania nanotubes on osteoblast functions. *Biomaterials.* 2010;31(19):5072–5082.
22. Santhosh S, Balasivanandha Prabu S. Thermal stability of nano hydroxyapatite synthesized from sea shells through wet chemical synthesis. *Mater Lett.* 2013;97:121–124.
23. Han CM, Lee EJ, Kim HE, et al. The electron beam deposition of titanium on polyetheretherketone (PEEK) and the resulting enhanced biological properties. *Biomaterials.* 2010;31(13):3465–3470.
24. Wennerberg A, Albrektsson T. On implant surfaces: a review of current knowledge and opinions. *Int J Oral Maxillofac Implants.* 2010; 25(1):63–74.
25. Gittens RA, McLachlan T, Olivares-Navarrete R, et al. The effects of combined micron-/submicron-scale surface roughness and nanoscale features on cell proliferation and differentiation. *Biomaterials.* 2011; 32(13):3395–3403.
26. Zhao G, Raines A, Wieland M, Schwartz Z, Boyan B. Requirement for both micron- and submicron scale structure for synergistic responses of osteoblasts to substrate surface energy and topography. *Biomaterials.* 2007;28(18):2821–2829.
27. Tarafder S, Bodhak S, Bandyopadhyay A, Bose S. Effect of electrical polarization and composition of biphasic calcium phosphates on early stage osteoblast interactions. *J Biomed Mater Res B Appl Biomater*. 2011;97(2):306–314.
28. Abe Y, Okazaki Y, Hiasa K, et al. Bioactive surface modification of hydroxyapatite. *Biomed Res Int*. 2013;2013:626452.
29. Györgyey Á, Ungvári K, Kecskeméti G, et al. Attachment and proliferation of human osteoblast-like cells (MG-63) on laser-ablated titanium implant material. *Mater Sci Eng C Mater Biol Appl.* 2013;33(7): 4251–4259.
30. Tan H, Guo S, Yang S, Xu X, Tang T. Physical characterization and osteogenic activity of the quaternized chitosan-loaded PMMA bone cement. *Acta Biomater.* 2012;8(6):2166–2174.
31. Altankov G, Grinnell F, Groth T. Studies on the biocompatibility of materials: fibroblast reorganization of substratum-bound fibronectin on surfaces varying in wettability. *J Biomed Mater Res.* 1996;30(3): 385–391.
32. Anselme K, Ponche A, Bigerelle M. Relative influence of surface topography and surface chemistry on cell response to bone implant materials. Part 2: biological aspects. *Proc Inst Mech Eng H.* 2010;224(12): 1487–1507.
33. Cai L, Guinn AS, Wang S. Exposed hydroxyapatite particles on the surface of photo-crosslinked nanocomposites for promoting MC3T3 cell proliferation and differentiation. *Acta Biomater.* 2011;7(5): 2185–2199.
34. Lincks J, Boyan BD, Blanchard CR, et al. Response of MG63 osteoblast-like cells to titanium and titanium alloy is dependent on surface roughness and composition. *Biomaterials.* 1998;19(23):2219–2232.
35. Meyer U, Büchter A, Wiesmann HP, Joos U, Jones DB. Basic reactions of osteoblasts on structured material surfaces. *Eur Cell Mater.* 2005;9: 39–49.
36. Liu Y, Cooper PR, Barralet JE, Shelton RM. Influence of calcium phosphate crystal assemblies on the proliferation and osteogenic gene expression of rat bone marrow stromal cells. *Biomaterials.* 2007;28(7): 1393–1403.
37. Kruger EA, Im DD, Bischoff DS, et al. In vitro mineralization of human mesenchymal stem cells on three-dimensional type I collagen versus PLGA scaffolds: a comparative analysis. *Plast Reconstr Surg.* 2011; 127(6):2301–2311.
38. Webster TJ, Ergun C, Doremus RH, Siegel RW, Bizios R. Enhanced functions of osteoblasts on nanophase ceramics. *Biomaterials.* 2000; 21(17):1803–1810.